Density functional study of the monocationic allopurinol tautomers

ARTICLE *in* JOURNAL OF MOLECULAR STRUCTURE THEOCHEM · JUNE 2000

Impact Factor: 1.37 · DOI: 10.1016/S0166-1280(00)00358-4

ELSEVIER

Journal of Molecular Structure (Theochem) 504 (2000) 105–118

THEO CHEM

www.elsevier.nl/locate/theochem

Density functional study of the monocationic allopurinol tautomers

R. Villegas-Ortega[a], M.E. Costas[a,*], R. Acevedo-Chávez[b]

[a]*Facultad de Química, Universidad Nacional Autónoma de México, México 04510 DF, Mexico*
[b]*Centro de Química, Instituto de Ciencias, B. Universidad Autónoma de Puebla, Apartado Postal 1613, Puebla, Mexico*

Abstract

The chemical and physicochemical properties of the purine isomer allopurinol have been subject of study from experimental and theoretical points of view. In this paper, the density functional theory study of allopurinol^{1+} was carried out. Full geometry optimization and energy calculations for the 16 possible tautomers were performed. The sequence of the three most stable species is independent of the functionals and basis sets explored. Several molecular and electronic structure properties of K257, cE27 and K125 tautomers were calculated. Thermodynamic parameters concerning the heterocyclic protonic transfer and tautomeric processes were also obtained. These were employed to calculate the theoretical IR vibrational spectrum of allopurinol^{1+} in gas phase, and the assignment of vibrational modes for the most stable K257 tautomer was carried out. The theoretical properties of K257 are compared with those of neutral allopurinol. Both are matched with those of purine derivative hypoxanthine at the same protonation levels. Common and different features are found, which are compared with those inferred from the chemical and physicochemical behavior experimentally shown by the two isomers in condensed phase.

Keywords: Allopurinol; Purine isomer; Tautomerism; DFT calculations

1. Introduction

Xanthine oxidase (X.O., EC.1.2.3.2) is a very complex metalloenzyme which catalyzes the oxidation of purine derivative hypoxanthine to yield xanthine. This oxidation product also acts as a further substrate of the enzyme, and its oxidation leads to uric acid, which is the final product in the human-purines' catabolism [1]. Defects in several of these biological processes can result in a level increase of uric acid, and eventually to deposition of uric acid salts in joints. The disease associated with this process is known as gout [2], and is clinically treated with the purinic isomer [3,4] and antihyperuricemic drug allopurinol (Fig. 1).

Numerous efforts involving chemical, structural and spectroscopic studies have been carried out in order to gain insight on the nature and properties of the heterocycle–X.O. catalytic site interactions. Nevertheless the great advances in the knowledge of the nature and structural features of the Mo catalytic center [5–21], and also of the reaction mechanisms [22–59], several problems remain open up to the present date.

One of those efforts is the one related with the knowledge of the physicochemical and chemical properties of purine-type substrates and inhibitors of X.O. In this context, we have carried out theoretical studies of the substrate hypoxanthine [60–64]. These show a great correspondence between the trends of the

* Corresponding author.
E-mail address: costas@zenon.pquim.unam.mx (M.E. Costas).

0166-1280/00/$ - see front matter
PII: S0166-1280(00)00358-4

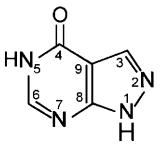

Fig. 1. Schematic drawing of neutral allopurinol (1-H pyrazolo [3,4-d] pyrimidin-4-one) in its *N*(1)–H/*N*(5)–H ketonic tautomeric form.

predicted theoretical properties and those inferred from the heterocyclic experimental behavior, both belonging to hypoxanthine–Lewis acid chemical interactions in different heterocyclic protonation states and tautomeric and isomeric forms. As part of our research program, we have performed theoretical studies of allopurinol, because of its pharmacological relevance and isomeric character with respect to hypoxanthine. From these studies, a concordance between the theoretical and the experimental properties has been found [60,65] for neutral allopurinol.

The rationalized common features and differences in the physicochemical and chemical behavior between neutral hypoxanthine and allopurinol, prompted us to extend the theoretical studies of these heterocycles in different protonation levels. In this communication, several theoretical properties for the energetically most favored monocationic allopurinol tautomers are presented and discussed. Those properties are employed to interpret some features of the behavior experimentally shown by monocationic allopurinol. Finally, some common features and differences in the physicochemical and chemical behavior for monocationic hypoxanthine and allopurinol are commented from the experimental and theoretical points of view.

2. Methodology

Geometry optimizations and total molecular energy calculations (including zero-point energy) of the 16 possible monocationic allopurinol tautomeric forms, were performed at the density functional theory level with the Becke–Perdew (BP86) exchange-correlation functional [66,67] and the DZVP basis set [68], by using the standard procedure in GAUSSIAN94 [69]. Calculations with a larger basis set (6-31G**) and the B3LYP functional were also done for the three energetically most stable tautomers predicted at the BP86/DZVP level. For the three calculation levels, the same sequence for the three energetically most stable tautomers was found. Also, we have found the BP86/DZVP calculation level reliable in accordance with a previous theoretical analysis of the experimental IR spectrum of neutral hypoxanthine [61]. Additionally, by employing the BP86/DZVP, B3LYP/DZVP and BP86/6-31G** calculation levels, the energetically most stable tautomer identity and its properties for anionic [64] and cationic [62,63] hypoxanthine, and neutral allopurinol [65], are found to be the same. We have thus decided to continue our systematic study of allopurinol in its ionic forms by employing the BP86/DZVP level.

The optimized structures of neutral allopurinol tautomeric forms [65] were used as input data for geometry optimizations of all the monocationic forms by addition of one H^+. For the enolic tautomers, a number of initial OH-group conformations was selected, and the *cis*- and *trans*-isomers always converged to the same respective structure. Criteria for geometry optimization and SCF-convergence were 10^{-7} hartree/bohr and 10^{-9} hartree, respectively. Frequency calculations were done to establish the stationary points nature found by geometry optimizations. All the 16 tautomers were stationary points in the geometry optimization procedure, and none showed imaginary frequencies in the vibrational analysis.

Single-point calculations by employing GAUSSIAN92 [70] with the same functional and basis set, were performed for the optimized structures of the three energetically most stable allopurinol^{1+} tautomers in order to visualize their properties. The difference in the SCF-energy with respect to the value obtained with GAUSSIAN94 was of 10^{-8} hartree in all cases. Visualization of the several calculated properties was done with the Unichem program [71]. Single-point calculations with the Dgauss program [72] for the GAUSSIAN94 optimized geometries were also done to obtain the Mayer valence indices [73].

The calculated frequencies (as wave numbers) of the IR vibrational spectra were corrected with a scaling factor of 1.0054. This was obtained by comparing the theoretical IR ν(C=O) vibrational mode wave number (1725.6993 cm^{-1}) for the *N*(1)–H/*N*(7)–H neutral hypoxanthine tautomer in gas phase [61] with the experimental value (1735 cm^{-1})

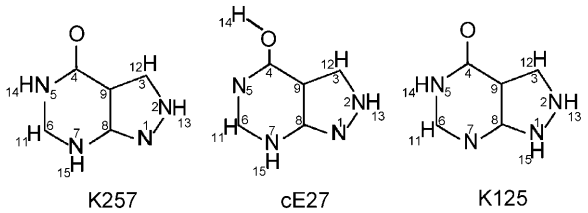

Fig. 2. Schematic drawing and numbering sequence for the three energetically most stable allopurinol^{1+} tautomeric forms. K, ketonic; E, enolic; c, OH group *cis*-configuration relative to *N*(5) atom; numbers in tautomeric abbreviations correspond to H atoms positions.

[74]. Vibrational normal modes assignment for the different cationic forms was done by visualizing them at each frequency value with the XMol program [71]. Frequency calculations were done at 298.15 and 500 K to obtain the Gibbs free energy thermal corrections; the contributions to these corrections were calculated within the rigid-rotor/harmonic-oscillator/ideal-gas approximation with the rotational constants and harmonic frequencies using the standard methods of statistical mechanics [75]. The $\bar{G}$ values were employed to calculate both the $\Delta\bar{G}$ for certain heterocyclic protonic transfer processes and the constants of tautomeric equilibria at those temperatures. First vertical ionization potentials and electron affinities were obtained as the SCF-energy differences between the resulting radicals and the starting monocationic forms both at the same respective optimized structures.

The calculations were done on a Origin-SGI 2000 and a CRAY-YMP4/464 supercomputers (at DGSCA, UNAM) and a R4400-SGI workstation (at FQ, UNAM).

Table 1
Total molecular energy differences (ΔE, kcal/mol) for the three energetically most stable monocationic allopurinol tautomeric forms, by employing three different DFT calculation levels. ΔE is referred to K257 species. ZPE is included in the respective total molecular energies

Tautomer	ΔE		
	BP86/DZVP	BP86/6-31G**	B3LYP/DZVP
cE27	2.46	1.55	2.13
K125	4.95	5.10	4.24

3. Results and discussion

3.1. Relative energetic stability

Among the 16 possible monocationic allopurinol tautomers, K257, cE27 and K125 (Fig. 2) are the three energetically more favored ones.

Independently of the functionals and basis sets here explored, K257 is the comparatively most stable species. Table 1 shows the relative energetic stabilities for these three tautomers. The remaining 13 species show energetic differences higher than 8.5 kcal/mol at the BP86/DZVP level.

The tautomeric features (and the OH-group configuration in the enolic form) strongly influence the energetic stability of monocationic heterocycles. In this stability, repulsive intramolecular interactions appear to play a critical role. From the analysis of the tautomeric features and the stabilities for all the possible tautomers, a correspondence between the descending energetic stability and the ascending repulsive intramolecular interactions inferred is found. This also is proposed to exist in the K125 tautomer; its relative energetic stability could be associated with protonation of the neighboring *N*(1) and *N*(2) sites in the pyrazolic moiety. The first two energetically most stable species show protonation of *N*(2) and *N*(7) atoms, their difference resting in the ketonic (K257) and enolic (cE27) characters. From the relative energetic stability results, the main contribution of K257 species to the tautomeric population of monocationic allopurinol in gas phase can be proposed.

When these theoretical results are attempted to be extended to the tautomeric analysis under increased solvent dielectric constant, the electric dipole moment (EDM) of the tautomers value must be considered. In

Table 2
Electric dipole moment (μ), HOMO and LUMO energies, and first vertical ionization potential and electron affinity for the three energetically most stable allopurinol^{1+} tautomers

Tautomer	μ (D)	HOMO (eV)	LUMO (eV)	IP (eV)	EA (eV)
K257	4.31	−11.20	−7.65	14.01	−4.94
cE27	0.76	−11.20	−7.85	13.99	−5.19
K125	5.77	−10.81	−7.56	13.75	−4.92

this aspect, good agreement between experimental heterocyclic tautomeric population in solution and both energetic and EDM properties (from theoretical calculations in gas phase) has been found [60–65]. As a consequence, a monocationic allopurinol tautomeric population theoretical prediction in solution can be made: between the first two energetically most stable K257 and cE27 tautomers, the species showing the higher EDM value in isolated state will be the comparatively more stabilized form in solutions with increased dielectric constant.

The EDM values are shown in Table 2. These let us suggest the predominant contribution of K257 to the tautomeric population of monocationic allopurinol in aqueous solution.

When this theoretical suggestion is compared with the experimental results [76,77] concerned with the characterization of monocationic allopurinol in condensed phase, a full agreement is found. In these, K257 is established as the unique existing allopurinol^{1+} tautomer in solid state. Also in this context, an assignment of the experimental electronic spectra of monocationic allopurinol in acidic aqueous solution has been made [78]. In such study, theoretical calculations at the semi-empirical level of electronic transitions for some allopurinol^{1+} species lead to the suggestion about the participation of either K257 or a *N*(2)–H/*N*(7)–H enolic form in the corresponding fluorescence excitation spectrum. Our theoretical analysis and its correspondence with the existence of K257 in the solid state, support the suggestion about the preponderance of this same tautomer in allopurinol^{1+} aqueous solution.

The allopurinol-H^+ thermodynamic stability constants study in aqueous solution and assignment of the protonic dissociation sites, have been subject of research by several groups [76–81]. In these studies, disagreement in both protonic dissociation stability constants (as pK_a values) and identity of protonic dissociation sites is found. Considering again our theoretical analysis and its concordance with the commented experimental information, it is possible to propose here the *N*(7) atom as the electron-donor site mainly involved in the protonic dissociation (p$K_a = 1.348$) of allopurinol^{1+} in aqueous solution [80]. This process yields neutral allopurinol as a mixture of *N*(1)–H/*N*(5)–H and *N*(2)–H/*N*(5)–H ketonic tautomers [60,65], the contribution of the first one being increased with the solvent dielectric constant.

3.2. Structural and chemical bonding parameters

Previous theoretical calculations carried out on neutral allopurinol [60,65] show a close relationship between tautomerism and molecular structure parameters. This has also been experimentally found when the heterocycle is coordinated to metallic centers in either the *N*(1)–H/*N*(5)–H or *N*(2)–H/*N*(5)–H ketonic forms [82]. Here, it is also important to note the remarkable concordance between the theoretical [65] and the experimental [4] structural properties for free neutral allopurinol in its *N*(1)–H/*N*(5)–H form.

When neutral allopurinol is monoprotonated, theoretical structural changes are observed. When the theoretical properties of the most stable neutral *N*(1)–H/*N*(5)–H (K15) form and the monocationic *N*(2)–H/*N*(5)–H/*N*(7)–H (K257) form are compared, the same noticeable correspondence between changes in both internuclear distances and angles, and the protonation state of groups involving *N* sites is deduced. For both heterocycles (K15 and K257) a typical ketonic character is suggested. When the theoretical structural properties of K257 are compared with the experimental ones [76], a great similarity for the values of the angles involving endocyclic groups is detected. Both structures also show a

Table 3
Internuclear distances (Å) and angles (°) of optimized structures for the three energetically most stable K257, cE27 and K125 monocationic allopurinol tautomers

Group	K257	cE27	K125
Internuclear distances			
N1–N2	1.365	1.368	1.370
N2–C3	1.359	1.354	1.354
C3–C9	1.404	1.412	1.400
C9–C4	1.452	1.422	1.468
C4–N5	1.487	1.353	1.442
N5–C6	1.338	1.330	1.367
C6–N7	1.336	1.358	1.325
N7–C8	1.398	1.382	1.354
C8–N1	1.335	1.336	1.368
C8–C9	1.425	1.433	1.423
C4–O	1.215	1.326	1.221
C6–H11	1.094	1.095	1.096
C3–H12	1.090	1.090	1.091
N2–H13	1.025	1.026	1.025
H14	N5–1.029	O–0.991	N5–1.028
H15	N7–1.027	N7–1.028	N1–1.026
Angles			
N1–N2–C3	115.24	116.02	110.28
N2–C3–C9	105.30	104.80	107.25
C3–C9–C8	103.56	103.72	107.05
C9–C8–N1	113.92	113.64	107.08
C8–N1–N2	101.98	101.82	108.33
C9–C4–N5	109.49	120.94	109.16
C4–N5–C6	126.92	119.25	125.86
N5–C6–N7	121.12	124.60	125.47
C6–N7–C8	119.14	118.55	112.23
N7–C8–C9	121.40	119.39	128.23
C8–C9–C4	121.94	117.26	119.05
C3–C9–C4	134.50	139.02	133.91
N1–C8–N7	124.68	126.96	124.68
N5–C4–O	118.94	118.79	122.16
C9–C4–O	131.57	120.27	128.68
N5–C6–H11	119.96	118.77	116.18
N7–C6–H11	118.92	116.63	118.35
N2–C3–H12	123.05	122.95	121.18
C9–C3–H12	131.65	132.25	131.57
H13	N1–N2–117.71	N1–N2– 117.37	N1–N2– 120.78
H13	C3–N2–127.05	C3–N2– 126.62	C3–N2– 128.94
H14	C4–N5–114.40	C4–O–108.46	C4–N5– 114.93
H14	C6–N5–118.68	–	C6–N5– 119.21
H15	C6–N7–120.60	C6–N7– 120.98	N2–N1– 122.37
H15	C8–N7–120.26	C8–N7– 120.46	C8–N1–129.29

common internuclear distances pattern. The theoretical ketonic character suggested before for K257 is supported through the respective experimental structural parameters. Here it is interesting to comment that although intermolecular forces in solid allopurinol^{1+} exist, its global network features are successfully reproduced by the theoretical calculations done considering full geometry optimization in isolated state.

Tautomerism also influences the heterocyclic structural properties in the monocationic state, in the

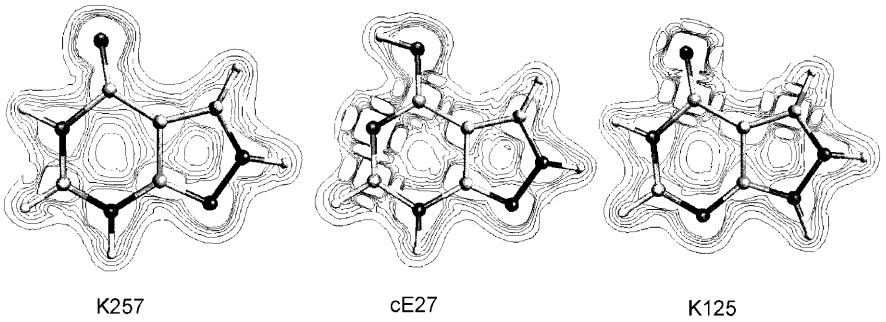

Fig. 3. Total electronic charge density contour maps at the molecular plane (0.05–0.30 e/Å^3 range, changes in 0.05 units) for the three energetically most stable K257, cE27 and K125 monocationic allopurinol tautomers.

same way as it does in neutral allopurinol. This is clearly observed for the K257, cE27 and K125 tautomers. Table 3 shows the theoretical structural data for these tautomers.

For the K257, cE27 and K125 allopurinol^{1+} tautomers, the first two species are completely planar under full geometry optimization. Only K125 shows deviations of ca. 0.1° for three of its dihedral angles. The small experimental deviations of planarity for K257 in the solid state are suspected to be associated with the existing packing forces in the crystalline lattice.

The theoretical and experimental studies [60–64,82] done on the isomer hypoxanthine, show an analog concordance between structural properties and both protonic state and tautomeric forms. Related heterocycles have also shown this correspondence [83].

The same tautomerism and protonation-structural properties relationship commented before is also observed in the total electronic charge density (TECD) and the Mayer valence-occupied indices properties. K257, cE27 and K125 show a comparatively higher TECD symmetry when compared with the TECD of K15 and K25 forms of neutral allopurinol [65]. Thus, a comparatively higher electronic charge density distribution throughout the heterocyclic network of those tautomers is proposed. Fig. 3 shows the TECD contour maps for K257, cE27 and K125.

The TECD features for the C–O group in K257 support the ketonic character suggested before, and the Mayer indices are in full concordance with this property. Table 4 shows the Mayer indices for K257, cE27 and K125.

Previous theoretical studies carried out on cationic hypoxanthine [62–64] show an analog behavior for the TECD and Mayer indices properties when the neutral purine derivative [60,61] is protonated.

Table 4
Mayer valence-occupied indices of the atoms corresponding to the three energetically most stable K257, cE27 and K125 monocationic allopurinol tautomers

Atom	K257	cE27	K125
N1	3.021	3.010	3.323
N2	3.432	3.450	3.367
C3	3.746	3.737	3.757
C4	4.110	4.044	4.136
N5	3.369	3.207	3.337
C6	3.846	3.920	3.907
N7	3.459	3.450	3.165
C8	3.926	3.927	3.907
C9	3.885	3.911	3.862
O	2.318	2.228	2.294
H11	0.876	0.878	0.883
H12	0.876	0.877	0.869
H13	0.778	0.776	0.775
H14	0.789	0.763	0.799
H15	0.785	0.791	0.792

3.3. Electric dipole moment and molecular electrostatic potential

Fig. 4 shows the electric dipole moment (EDM) vector together with the molecular electrostatic potential (MEP) contour map for K257, cE27 and K125 allopurinol^{1+} tautomers.

The MEP pattern is strongly dependent on the

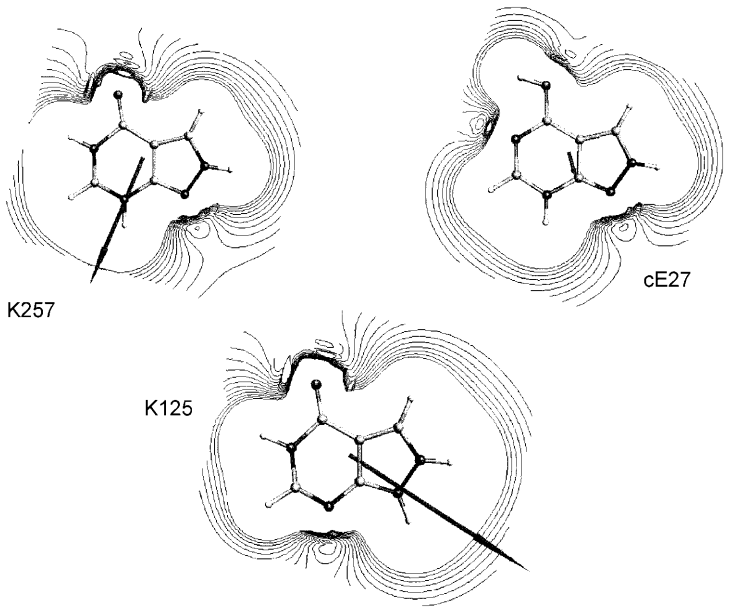

Fig. 4. Electric dipole moment (*D*) together with the molecular electrostatic potential contour map (kcal/mol) for K257 (+ 35 to + 100), cE27 (+ 40 to + 100) and K125 (+ 35 to + 100) allopurinol^{1+} tautomers. Both properties are at the molecular plane level. EDM vector is referred to the molecular center of mass; the arrow head points to the positive tip. MEP is referred to a positive charge as a probe; the inner contour corresponds to the + 100 level.

allopurinol^{1+} tautomeric form. The EDM properties show correspondence with those of the MEP. In the monocationic state, allopurinol shows positive (repulsive) MEP values. However, when this property is analyzed in detail, some features can be drawn. For the highest MEP level selected, all the protonated regions show the respective isocontour at longer distances than those for the deprotonated ones. When the repulsive MEP level is decreased, a noticeably higher increase of such distances for the former ones is observed. These MEP properties let us suspect that, for example in K257, the *O* and *N*(1) sites would be the comparatively less unfavored atoms to be involved in additional electrostatic interactions with Lewis acids. Fig. 5 shows the + 60 kcal/mol isosurface for the K257 tautomer.

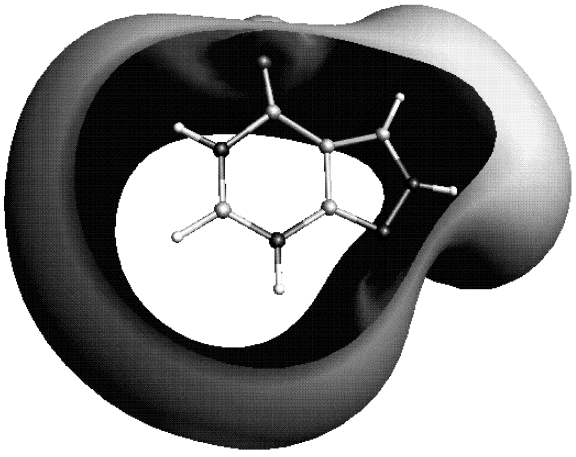

Fig. 5. Repulsive MEP isosurface at the + 60 kcal/mol level for the K257 allopurinol^{1+} tautomer.

This possibility would be supported through the participation of *N*(1) as metallic coordinating site in a K257 allopurinol^{1+}–Cu(II) coordination compound [77]. Allopurinol^{2+} has not been experimentally detected up to the present day. Allopurinol shows a comparatively lower pK_a value (1.348) for the allopurinol^{1+} ⇔ allopurinol^{0} + H^{+} equilibrium as compared with the homologue one (ca. 2.0) for its isomer hypoxanthine [80]. The negative (−3.3 to −3.6) pK_a value [62–64] is found for the hypoxanthine^{2+} ⇔ hypoxanthine^{1+} + H^{+} equilibrium. This let us consider a comparatively higher negative

Fig. 6. (a) HOMO; and (b) LUMO wave functions (isosurfaces at the ±0.025 level) for the allopurinol^{1+} K257 tautomer.

pK_a value for allopurinol^{2+}, and thus a comparatively higher H^+ concentration in solution for the allopurinol^{2+} stabilization than that employed experimentally [80].

The isomer hypoxanthine in monocationic state shows an analog MEP behavior than that discussed here for allopurinol^{1+}. The stabilization [62–64] in very acid aqueous solution of the K1379 hypoxanthine^{2+} tautomer supports the theoretical MEP analysis previously made for the K179 hypoxanthine^{1+} species, and give us confidence about the one done for allopurinol^{1+}, in particular for the K257 tautomer.

3.4. HOMO and LUMO wave function properties

Table 2 shows the HOMO and LUMO energies for the first three energetically most stable allopurinol^{1+} tautomers. When the K257 frontier MO's energies are compared with those for the most stable neutral allopurinol species [65], the former one shows higher negative values. From these data, allopurinol^{1+} is suggested to show comparatively lower Lewis base and higher Lewis acid properties than those for neutral allopurinol.

An analog theoretical behavior has been deduced [63] for the isomer hypoxanthine in the K179 monocationic state. The chemical reactivity decrease (towards transitional Lewis acids) experimentally shown by allopurinol [82] and hypoxanthine [64,82] under monoprotonation (i.e. monocationic states) would be in agreement with such frontier MO's properties for these isomers.

The corresponding energetically most favored tautomers of neutral (K15) [65] and monocationic (K257) allopurinol show the same molecular distribution of their respective Π-type HOMO and LUMO wave functions. Those for K257 are shown in Fig. 6.

The same HOMO molecular distribution has been found for the isomer hypoxanthine, independently of its protonation state and the respective tautomeric or isomeric forms [61–64]. From the allopurinol wave functions features, it is possible to propose that the *O* site and those *N* atoms more favored as potential Π-type electron-donor and electron-acceptor sites would keep such capabilities independently of both the heterocyclic protonation state (i.e. neutral or monocationic) and the corresponding tautomeric forms.

3.5. First vertical ionization potential and electron affinity

These properties belong to the energy differences for the processes: monocationic species ($S = 0$, singlet ground state) → dicationic species ($S = 1/2$, doublet ground state) and monocationic species ($S = 0$, singlet ground state) → neutral species ($S = 1/2$, doublet ground state), respectively. The ionization potential (IP) and electron affinity (EA) values for K257, cE27 and K125 allopurinol^{1+} tautomers are shown in Table 2. The negative EA values are associated with the energetic stabilization of tautomers upon their reduction. When the IP and EA values for K257 are compared with those for K15 in neutral allopurinol [65], it is observed that the monocationic tautomer shows higher positive IP (+14.01 eV vs. +7.49 eV) and higher negative EA negative (−4.94 eV vs. +0.25 eV) values. As a consequence, K257 is postulated here to show a comparatively higher reluctance to oxidation (lower Lewis base character) and a higher affinity to reduction

Table 5
$\Delta\bar{G}$ (kcal/mol) values at 298.15 and 500 K for selected monoprotonation processes of neutral allopurinol and yielding monocationic species

Protonation process	$\Delta\bar{G}$ (kcal/mol)	
	298.15 K	500 K
K25 → K257	−214.83	−223.13
K15 → K125	−206.76	−215.43
K25 → K125	−210.18	−218.89

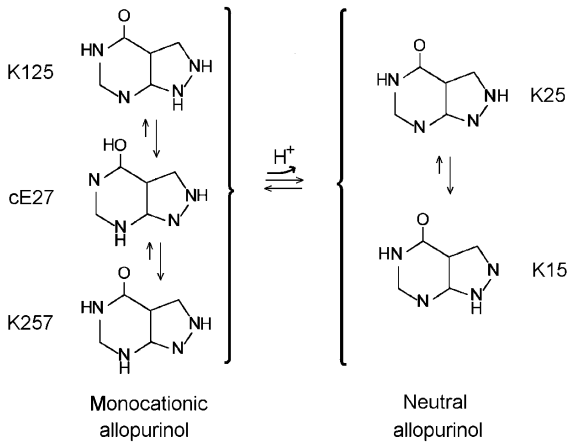

Fig. 7. Scheme of the protonic transfer equilibrium for monocationic and neutral allopurinol, and involving the respective thermodynamically more favorable species in gas phase.

(higher Lewis acid character) than K15. This postulate is in agreement with the frontier MO energetic analysis made in Section 3.4. An analog theoretical behavior has been deduced [63] from the IP (+ 13.56 eV vs. + 8.73 eV) and EA (−4.53 eV vs. + 0.5 eV) values for the isomer hypoxanthine K179 monocationic tautomer as compared with the K17 neutral species. The theoretical behavior of the IP and EA values for both monocationic isomers is also in agreement with their decreased chemical reactivity commented before.

The K257 HOMO and LUMO are considered to be the MO mainly involved in the Redox processes here explored. When the theoretical properties of the frontier MO wave functions and the IP and EA values are considered, it seems that in allopurinol the identity of the more favored atoms in the Π-type electronic charge transfer processes previously explored, is independent of the heterocyclic protonic state (neutral or monocationic) and its tautomerism. It is only their energetic accessibility that shows differences.

3.6. Gibbs free energy differences for heterocyclic protonic transfer processes

In order to analyze some thermodynamic features of heterocyclic protonic transfer in which the three energetically most stable allopurinol^{1+} tautomers could be involved, the $\Delta\bar{G}$ values for selected processes of the type: neutral allopurinol species ⇔ monocationic allopurinol species and monocationic tautomer (i) ⇔ monocationic tautomer (j) were calculated. Table 5 shows theoretical values for some of the selected processes.

From Table 5 the thermodynamically favorable character for neutral allopurinol monoprotonation and yielding monocationic species is deduced. This thermodynamic spontaneity in gas phase is slightly increased with temperature. Using the $\bar{G}$ values of K257 and cE27 species, $\Delta\bar{G} = +2.58$ kcal/mol (298.15 K) for the K257 → cE27 tautomerism process

Table 6
(a) $\Delta\bar{G}$ (kcal/mol) values and equilibrium constants (K_{eq}) at 298.15 and 500 K for tautomeric processes which involve the first three most stable allopurinol^{1+} tautomers in gas phase; and (b) mole fraction (x_i) values at 298.15 and 500 K for the K257, cE27 and K125 allopurinol^{1+} tautomers in gas phase

Tautomeric process	298.15 K		500 K	
	$\Delta\bar{G}$ (kcal/mol)	K_{eq}	$\Delta\bar{G}$ (kcal/mol)	K_{eq}
K257 → cE27	+ 2.58	0.01284	+ 2.77	0.0613
K257 → K125	+ 4.65	0.00039	+ 4.24	0.0140

(b)

Tautomer	x_i	
	298.15 K	500 K
K257	0.986943	0.929973
cE27	0.012672	0.057007
K125	0.000385	0.01302

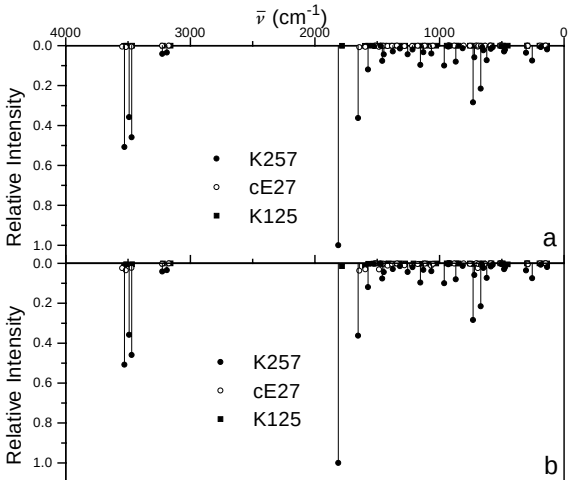

Fig. 8. Theoretical IR vibrational spectrum of allopurinol^{1+} in gas phase, considering the relative contributions at: (a) 298.15 K; and (b) 500 K of K257, cE27 and K125 tautomers.

is obtained. This is also found from the combination of the $\Delta\bar{G}$ values for the K27 → cE27 and K27 → K257 protonation processes. These results let us suggest the relatively higher σ-type basicity (toward H^+) of *N*(5) compared with that for the exocyclic *O* site in allopurinol^{1+} species. In this context, the theoretical $\Delta\bar{G}$ values for the K25 → K257 and K25 → K125 protonation processes, let us obtain $\Delta\bar{G} = +4.65$ kcal/mol (298.15 K) for the K257 → K125 tautomerization. This $\Delta\bar{G}$ value allows us to suggest the comparatively higher *N*(7)–H thermodynamic stability in comparison with that for *N*(1)–H under simultaneous protonation of *N*(2) and *N*(5) sites in allopurinol^{1+} species. The $\Delta\bar{G}$ values for the tautomeric processes let us also consider the comparatively higher thermodynamic stability in gas phase of K257 allopurinol^{1+} tautomer, both at 298.15 and 500 K, this last being the approximate neutral allopurinol experimental sublimation temperature [65]. The theoretical $\Delta\bar{G}$ values analysis supports the considerations we have made concerned with the comparatively higher stability of K257 species from the energetic point of view.

In addition, the respective monoprotonation processes: K25, K27 → K257 were explored. From the $\Delta\bar{G}$ values obtained, the noticeably higher σ-type basicity of *N*(5) than that for *N*(7) is inferred. On the other hand, the K15, K25, K12 → K125

Table 7
Corrected wave numbers ($\bar{\nu}$, cm^{-1}), intensities (*I*, kM/mol), and vibrational modes assignment of allopurinol^{1+} K257 tautomer theoretical IR vibrational absorptions

$\bar{\nu}$	*I*	Assignment
3528.86	234.36	ν *N*(2)–H, ν *C*(3)–H, ν N–H
3491.30	165.26	ν *N*(5)–H/ν *N*(7)–H, ν *C*(6)–H/ν *N*(2)–H
3471.15	212.01	ν *N*(5)–H/ν *N*(7)–H, ν *C*(6)–H/ν *N*(2)–H
3225.20	18.98	ν *C*(3)–H, ν *N*(2)–H
3187.78	16.05	ν *C*(6)–H, ν *N*(5)–H/ν *N*(7)–H
1812.67	461.58	ν C=O, rings vib., δ *N*(5)–H
1652.73	167.52	*C*(6)–H vib., rings vib., C–H vib./N–H vib./C=O vib.
1573.69	55.19	*N*(7)–H vib./*C*(6)–H vib., rings vib., C–H vib./N–H vib./ν C=O
1526.33	0.93	*N*(7)–H vib., rings vib., C–H vib./N–H vib./ν C=O
1471.42	0.20	*N*(7)–H vib., rings vib., C–H vib./N–H vib./C=O vib.
1458.98	35.19	*N*(2)–H vib., rings vib., C–H vib./*N*(5)–H vib../ν C=O
1446.65	20.36	*C*(3)–H vib./*N*(5)–H vib., rings vib., *N*(2)–H vib., C=O vib.
1373.87	13.34	*N*(5)–H vib./*C*(6)–H vib., rings vib., C–H vib./N–H vib./ν C=O
1316.99	6.81	*C*(3)–H vib., rings vib., *N*(2)–H vib., C=O vib.
1255.49	20.08	*C*(6)–H vib., rings vib., *N*(5)–H vib./*N*(7)–H vib.
1215.88	8.92	Rings vib., C–H vib., *N*(5)–H vib./*N*(7)–H vib., C=O vib.
1153.49	44.66	Rings vib., *N*(2)–H vib./*N*(5)–H vib., C=O vib.
1129.40	15.29	Rings vib., N–H vib., C=O vib.
1064.82	18.27	*C*(3)–H vib., rings vib., C=O vib.
962.07	46.17	Rings vib., C–H vib./*N*(2)–H vib., C=O vib.
929.22	2.38	*C*(3)–H vib., rings vib.
917.30[a]	0.04	*C*(6)–H vib., rings vib.
868.82	36.99	Rings vib., C=O vib.
813.61[a]	6.13	*C*(3)–H vib., rings vib., *N*(2)–H vib./C=O vib.
730.00[a]	131.12	*N*(5)–H vib., rings vib., *C*(3)–H vib., C=O vib.
719.94[a]	26.94	*N*(5)–H vib., rings vib., *N*(7)–H vib.
668.84[a]	99.51	*N*(2)–H vib., rings vib., *C*(3)–H vib.
657.34[a]	3.64	*N*(7)–H vib., rings vib., *N*(2)–H vib., C=O vib.
647.27	10.74	Rings vib., C=O vib.
620.56[a]	33.69	Rings vib., N–H vib., C=O vib.

Table 7 (*continued*)

$\bar{\nu}$	I	Assignment
587.19[a]	7.46	*N*(2)–H vib., rings vib., N–H vib., C–H vib., C=O vib.
571.90	3.68	Rings vib., C=O vib.
501.83	1.57	Rings vib., C=O vib.
481.44[a]	13.71	*C*(6)–H vib., rings vib., *N*(5)–H vib./*N*(7)–H vib., C=O vib.
474.04	9.63	Pyrimidinic ring vib.
304.97	16.38	Rings vib., C=O vib.
255.55[a]	34.61	Rings vib., C=O vib.
186.66[a]	3.31	Rings vib.
136.23[a]	8.64	Rings vib., C=O vib.

[a] Out of the molecular plane vibrations.

processes $\Delta\bar{G}$ values are in concordance with the comparatively higher σ-type basicity of *N*(5) than those for both *N*(1) and *N*(2) sites.

All the precedent $\Delta\bar{G}$ values let us propose a scheme for the allopurinol monocationic species ⇔ allopurinol neutral species protonic transfer equilibrium in gas phase. This is shown in Fig. 7.

When this scheme is compared with the proposition corresponding to the isomer hypoxanthine [62–64], common features and differences emerge. For both isomers, the respective thermodynamically most stable monocationic species are ketonic forms, which show protonation of the *N* site nearest to the carbonyl group. This feature is maintained in the respective most stable neutral forms [61,65]. The most stable K179 tautomer in hypoxanthine^{1+} shows full protonation of the imidazolic ring; the K179 protonic dissociation involves such five-membered ring. As a difference, in allopurinol^{1+} K257 tautomer, both the five- and six-membered rings show protonation (at *N*(2) and *N*(7) sites); the K257 protonic dissociation involves the *N*(7) atom of the pyrimidinic ring.

The extension of this $\Delta\bar{G}$ analysis to aqueous solution-allopurinol protonic transfer processes has to be done very carefully, because the acid–base properties and the dielectric constant of water as a solvent must be considered. In here, the thermodynamic stability of allopurinol^{1+} in gas phase has been deduced; in aqueous solution, allopurinol^{1+} is only thermodynamically favored at very high H^+ concentrations ($\geq 10^{-1.348}$ M). An analog theoretical $\Delta\bar{G}$ analysis has been previously made for the hypoxanthine monoacationic form [63], which is in concordance with the experimental physicochemical behavior of this heterocycle in aqueous solution [64].

It is important to point out that one must be very cautious when these σ-type basicities (toward H^+) are pretended to be used to perform an analysis of the heterocycle-transition metallic center (M^{n+}) chemical reactivity. At this respect, and in the same way as for the isomer hypoxanthine [64], there is no clear relationship between allopurinol-H^+ [76–81] and allopurinol-M^{n+} [76,77,80,82,84–94] thermodynamic stabilities for which a common heterocyclic electron-donor site is involved.

3.7. Tautomeric equilibria

An interesting aspect in this study concerns the evaluation of the tautomeric equilibrium constants (K_{eq}) taking into account the participation of the three thermodynamically most stable allopurinol^{1+} tautomers in gas phase. The K_{eq} values were calculated with the equation:

$$K_{eq} = \frac{[\text{Tautomer } i]}{[\text{K257}]} = e^{-\Delta\bar{G}/RT}$$

where $\Delta\bar{G}$ is the molar Gibbs free energy difference between tautomer *i* and K257. Table 6 shows the K_{eq} values at 298.15 and 500 K.

For a particular temperature value, a decreasing trend of the K_{eq} values with both the energetic and thermodynamic stabilities of tautomer *i* is found. For a particular tautomeric equilibrium, the K_{eq} values increase with temperature. For both temperatures the K_{eq} values let us suggest the predominant contribution of K257 to the tautomeric population of allopurinol^{1+} in gas phase. This is corroborated through the mole fraction values shown in Table 6.

3.8. IR vibrational spectroscopy

As part of our theoretical study of the allopurinol^{1+} properties, the calculation of the IR vibrational spectrum for K257, cE27 and K125 tautomers and the corresponding absorptions assignment were carefully done. We selected 298.15 and 500 K as the temperature values for which the theoretical spectral analysis of the allopurinol^{1+} tautomeric population in gas phase should be done, through the corresponding K257, cE27 and K125 mole fractions. For each

tautomer spectrum, the theoretical intensities of the absorptions were weighted by the correspondent mole fraction, and all the intensities of the three spectra were scaled relative to the highest intensity signal. The resulting theoretical IR vibrational spectra of allopurinol^{1+} considering the tautomeric contributions at both temperatures are shown in Fig. 8.

For both temperatures, the K257 tautomer shows the predominant spectral contribution. Table 7 shows the spectral data for the most stable K257 tautomer.

When this spectrum is compared with the IR spectral properties of the most stable neutral allopurinol tautomers [65], several differences are observed. One of these corresponds to the frequency of the most intense absorption which is mainly attributed to the ν C=O vibrational mode. For K15, $\bar{\nu} = 1747.00\ cm^{-1}$, whereas for K257, $\bar{\nu} = 1812.49\ cm^{-1}$. This increasing trend of $\bar{\nu}$ values for ν C=O with the heterocyclic protonation level has also been found for the isomer hypoxanthine [64].

4. Conclusions

With the results of the theoretical study carried out we can propose that in the monocationic state, allopurinol exists as essentially the K257 ketonic tautomer. The *N*(7) atom in the pyrimidinic ring is suggested as the site mainly involved in the K257 protonic dissociation. In contrast, hypoxanthine^{1+} isomer shows full protonation (K179 ketonic tautomer) of the five-membered ring. In this case, the *N*(7) atom in the imidazolic moiety appears as the site mainly involved in the K179 protonic dissociation. These theoretical suggestions are in concordance with the experimental evidence for both isomers.

Protonation level and tautomerism in allopurinol also influence several molecular and electronic structure theoretical properties, and trends for these are found when the allopurinol monocationic state is achieved. When these theoretical trends are compared with those of its isomer hypoxanthine, some differences are found, which have been partially supported through the inferred ones associated with the respective and experimental isomer^{1+} behavior reported up to the present date.

Among those are the ones concerning with the additional heterocyclic electrostatic interactions with Lewis acids, and the slightly lower Π-type reductor (Lewis base) character of K257 in comparison with K179.

The K257 and K179 IR spectral features are suggested to be an essential tool in the spectral analysis of both isomers in different protonation states, and which also includes chemical interactions with Lewis acids.

Acknowledgements

The authors are indebted to DGSCA, UNAM for the computer service facilities. This work was partially supported by DGAPA, UNAM through Grant no. ES-100597.

References

[1] L. Stryer, Biochemistry, 4th ed., Freeman, New York, 1995.
[2] C. Hansch, J. Chem. Educ. 51 (1974) 360 (and references therein).
[3] B.G. Hildrick, G. Shaw, J. Chem. Soc. C (1971) 1610.
[4] P. Prusiner, M. Sundaralingam, Acta Crystallogr. B 28 (1972) 2148.
[5] J.L. Johnson, B.E. Hainline, K.V. Rajagopalan, J. Biol. Chem. 255 (1980) 1783.
[6] T.R. Hawkes, G.N. George, R.C. Bray, Biochem. J. 218 (1984) 961.
[7] S.P. Cramer, R. Hille, J. Am. Chem. Soc. 107 (1985) 8164.
[8] S.P. Kramer, J.L. Johnson, A.A. Ribeiro, D.S. Millington, K.V. Rajagopalan, J. Biol. Chem. 262 (1987) 16 357.
[9] G.N. George, R.C. Bray, Biochemistry 27 (1988) 3603.
[10] R.C. Bray, Q. Rev. Biophys. 21 (1988) 299.
[11] R. Singh, J.T. Spence, G.N. George, S.P. Cramer, Inorg. Chem. 28 (1989) 8.
[12] R. Hille, G.N. George, M.K. Eidsness, S.P. Cramer, Inorg. Chem. 28 (1989) 4018.
[13] W.A. Oertling, R. Hille, J. Biol. Chem. 265 (1990) 17 446.
[14] G.L. Wilson, R.J. Greenwood, J.R. Pilbrow, J.T. Spence, A.G. Wedd, J. Am. Chem. Soc. 113 (1991) 6803.
[15] B.D. Howes, B. Bennett, A. Koppenhöfer, D.J. Lowe, R.C. Bray, Biochemistry 30 (1991) 3969.
[16] K.V. Rajagopalan, Adv. Enzymol. 64 (1991) 215.
[17] A.A. Eagle, L.J. Laughlin, C.G. Young, E.R.T. Tiekink, J. Am. Chem. Soc. 114 (1992) 9195.
[18] R.J. Greenwood, G.L. Wilson, J.R. Pilbrow, A.G. Wedd, J. Am. Chem. Soc. 115 (1993) 5385.
[19] M.G. Ryan, K. Ratnam, R. Hille, J. Biol. Chem. 270 (1995) 19 209.
[20] M.R. Bray, R.J. Deeth, Inorg. Chem. 35 (1996) 5720.

[21] A.A. Voityuk, K. Albert, N. Rosch, J. Am. Chem. Soc. 119 (1997) 3159.
[22] E.I. Stiefel, Proc. Natl. Acad. Sci. USA 70 (1973) 988.
[23] J.S. Olson, D.P. Ballou, G. Palmer, V. Massey, J. Biol. Chem. 249 (1974) 4363.
[24] R.C. Bray, The Enzymes 12 (1975) 299.
[25] E.I. Stiefel, Prog. Inorg. Chem. 22 (1977) 1.
[26] R.C. Bray, Adv. Enzymol. Relat. Areas Mol. Biol. 51 (1980) 107.
[27] R. Hille, V. Massey, Pharmacol. Ther. 14 (1981) 249.
[28] R.K. Robins, G.R. Revankar, D.E. O'Brien, R.H. Springer, T. Novinson, A. Albert, K. Senga, J.P. Miller, D.G. Streeter, J. Heterocycl. Chem. 22 (1985) 601.
[29] S.J.N. Burgmayer, E.I. Stiefel, J. Chem. Educ. 62 (1985) 943.
[30] R. Hille, V. Massey, in: T.G. Spiro (Ed.), Nucleic Acid–Metal Ion Interactions, vol. 7, Wiley, New York, 1985, p. 443.
[31] R. Hille, H. Sprecher, J. Biol. Chem. 262 (1987) 10 914.
[32] R. Hille, R.F. Anderson, J. Biol. Chem. 266 (1991) 5608.
[33] R. Cammack, A. Chapman, J. McCracken, J. Peisach, J. Chem. Soc., Faraday Trans. 87 (1991) 3203.
[34] D. Coucouvanis, A. Toupadakis, J.D. Lane, S.M. Koo, C.G. Kim, A. Hadjikyriacou, J. Am. Chem. Soc. 113 (1991) 5271.
[35] R. Hille, V. Massey, J. Biol. Chem. 266 (1991) 17 401.
[36] M.C. Walker, J.T. Hazzard, G. Tollin, D.E. Edmonson, Biochemistry 30 (1991) 5912.
[37] H.S.D. Naeff, M.C.R. Franssen, H.C. van der Plas, Recl. Trav. Chim. Pays-Bas 110 (1991) 139.
[38] Z. Xiao, C.G. Young, J.H. Enemark, A.G. Wedd, J. Am. Chem. Soc. 114 (1992) 9194.
[39] R. Radi, S. Tan, E. Prodanov, R.A. Evans, D.A. Parks, Biochim. Biophys. Acta 1122 (1992) 178.
[40] R. Hille, J.H. Kim, C. Hemann, Biochemistry 32 (1993) 3973.
[41] R. Hille, in: E.I. Stiefel, D. Coucouvanis, W.E. Newton (Eds.), Molybdenum Enzymes, Cofactors and Model Systems, ACS Symposium Series, vol. 535, ACS, Washington, DC, 1993, p. 22.
[42] M.S. Mondal, S. Mitra, Biochemistry 33 (1994) 10 305.
[43] G.A. Lorigan, R.D. Britt, J.H. Kim, R. Hille, Biochim. Biophys. Acta 1185 (1994) 284.
[44] T. Nishino, J. Biochem. 116 (1994) 1.
[45] R. Hille, Biochim. Biophys. Acta 1184 (1994) 143.
[46] R. Huber, P. Hof, R.O. Duarte, J.J.G. Moura, I. Moura, M.Y. Liu, J. LeGall, R. Hille, M. Archer, M.J. Romáo, Proc. Natl. Acad. Sci. USA 93 (1996) 8846.
[47] B.D. Howes, R.C. Bray, R.L. Richards, N.A. Turner, B. Bennett, D.J. Lowe, Biochemistry 35 (1996) 1432.
[48] R. Hille, Chem. Rev. 96 (1996) 2757.
[49] M.R. Bray, R.J. Deeth, J. Chem. Soc., Dalton Trans. (1997) 1267.
[50] G. Rastelli, L. Constantino, A. Albasini, J. Am. Chem. Soc. 119 (1997) 3007.
[51] B. Hernández, M. Orozco, F.J. Luque, J. Comput. -Aided Mol. Des. 11 (1997) 153.
[52] R.L. Richards, New J. Chem. 21 (1997) 727.
[53] R.C. Bray, D.J. Lowe, Trans. Biochem. Soc. 25 (1997) 762.
[54] M. Xia, P. Ilich, R. Hille, Trans. Biochem. Soc. 25 (1997) 768.
[55] D.J. Lowe, R.L. Richards, R.C. Bray, Trans. Biochem. Soc. 25 (1997) 774.
[56] P. Ilich, R. Hille, Inorg. Chim. Acta 263 (1997) 87.
[57] M.R. Bray, R.J. Deeth, J. Chem. Soc., Dalton Trans. (1997) 4005.
[58] M.J. Romáo, R. Huber, Struct. Bonding 90 (1998) 69.
[59] A.A. Voityuk, K. Albert, M.J. Romáo, R. Huber, N. Rösch, Inorg. Chem. 37 (1998) 176.
[60] M.E. Costas, E. Ramos, R. Acevedo-Chávez, Computational chemistry and chemical engineering, in: G. Cisneros, J.A. Cogordan, M. Castro, C. Wang (Eds.), Proceedings of the Third UNAM-CRAY Supercomputing Conference, Universidad Nacional Autónoma de México, 13–16 August 1996, World Scientific, Singapore, 1997, p. 182 (and references therein).
[61] M.E. Costas, R. Acevedo-Chávez, J. Phys. Chem. A 101 (1997) 8309 (and references therein).
[62] M.E. Costas, R. Acevedo-Chávez, J. Mol. Struct. (Theochem) 468 (1999) 39.
[63] M.E. Costas, R. Acevedo-Chávez, J. Mol. Struct. (Theochem) 489 (1999) 73.
[64] R. Acevedo-Chávez, M.E. Costas, Recent Research Developments in Physical Chemistry, 3 (1999) 23.
[65] M.E. Costas, R. Acevedo-Chávez, J. Comput. Chem. 20 (1999) 200 (and references therein).
[66] A.D. Becke, Phys. Rev. A 38 (1988) 3098.
[67] J.P. Perdew, Phys. Rev. B 33 (1986) 8822.
[68] N. Godbout, D.R. Salahub, J. Andzelm, E. Wimmer, Can. J. Chem. 70 (1992) 560.
[69] M.J. Frisch, G.W. Trucks, H.B. Schlegel, P.M.W. Gill, B.G. Johnson, M.A. Robb, J.R. Cheeseman, T. Keith, G.A. Petersson, J.A. Montgomery, K. Raghavachari, M.A. Al-Laham, V.G. Zakrzewski, J.V. Ortiz, J.B. Foresman, J. Cioslowski, B.B. Stefanov, A. Nanayakkara, M. Challacombe, C.Y. Peng, P.Y. Ayala, W. Chen, M.W. Wong, J.L. Andres, E.S. Replogle, R. Gomperts, R.L. Martin, D.J. Fox, J.S. Binkley, D.J. Defrees, J. Baker, J.P. Stewart, M. Head-Gordon, C. Gonzalez, J.A. Pople, GAUSSIAN94, Revision D.4, Gaussian, Pittsburgh, PA, 1995.
[70] M.J. Frisch, G.W. Trucks, H.B. Schlegel, P.M.W. Gill, B.G. Johnson, M.W. Wong, J.B. Foresman, M.A. Robb, M. Head-Gordon, E.S. Replogle, R. Gomperts, J.L. Andres, K. Raghavachari, J.S. Binkley, C. Gonzalez, R.L. Martin, D.J. Fox, D.J. Defrees, J. Baker, J.P. Stewart, J.A. Pople, GAUSSIAN92/DFT, Revision F.3, Gaussian, Pittsburgh, PA, 1993.
[71] UNICHEM 3.0, Cray Research, Eagan, MN, 1995 and Xmol, Version 1.3.1, Minnesota Supercomputer Center, Minneapolis, MN, 1993.
[72] DGAUSS 3.0.1/UC-3.0, Cray Research, Eagan, MN, 1991.
[73] I. Mayer, Int. J. Quantum Chem. 29 (1986) 477.
[74] G.G. Sheina, S.G. Stepanian, E.D. Rádchenko, Yu.P. Blagoi, J. Mol. Struct. (Theochem) 158 (1987) 275.
[75] D.A. McQuarrie, Statistical Mechanics, Harper & Row, New York, 1973.
[76] W.S. Sheldrick, P. Bell, Inorg. Chim. Acta 137 (1987) 181.
[77] W.S. Sheldrick, P. Bell, Z. Naturforsch B 42 (1987) 195.

[78] M.K. Shukla, P.C. Mishra, Spectrochim. Acta Part A 52 (1996) 1547.
[79] B.M. Lynch, R.K. Robins, C.C. Cheng, J. Chem. Soc. (1958) 2973.
[80] P.W. Linder, M.J. Stanford, D.R. Williams, J. Inorg. Nucl. Chem. 38 (1976) 1847.
[81] F. Bergmann, A. Frank, Z. Neiman, J. Chem. Soc., Perkin I (1979) 2795.
[82] R. Acevedo-Chávez, M.E. Costas, R. Escudero, Inorg. Chem. 35 (1996) 7430 (and references therein).
[83] R. Taylor, O. Kennard, J. Mol. Struct. 78 (1982) 1.
[84] W.S. Sheldrick, B. Günther, Inorg. Chim. Acta 151 (1988) 237.
[85] G. Hänggi, H. Schmalle, E. Dubler, Inorg. Chem. 27 (1988) 3131.
[86] G. Hänggi, H. Schmalle, E. Dubler, Acta Crystallogr. C 44 (1988) 1560.
[87] R. Acevedo-Chávez, N.B. Behrens, Transition Met. Chem. 15 (1990) 434.
[88] G. Hänggi, H. Schmalle, E. Dubler, Acta Crystallogr. C 47 (1991) 1609.
[89] W.S. Sheldrick, G. Heeb, Inorg. Chim. Acta 190 (1991) 241.
[90] G. Hänggi, H. Schmalle, E. Dubler, J. Chem. Soc., Dalton Trans. (1993) 941.
[91] C.M. Mikulski, M.E. Holman, G. Tener, T. Dobson, S. Eang, W. Welsh, Y. Nujoma, N.M. Karayannis, Transition Met. Chem. 18 (1993) 262.
[92] R. Acevedo-Chávez, M.E. Costas, R. Escudero-Derat, J. Solid State Chem. 113 (1994) 21.
[93] E. Dubler, G. Hänggi, Thermochim. Acta 234 (1994) 201.
[94] R. Acevedo-Chávez, M.E. Costas, R. Escudero-Derat, Spectral and magnetic studies of novel purine derivative and isomer-Cu(II) coordination compounds, unpublished results.